C. R. Chimie 22 (2019) 549–556

Contents lists available at ScienceDirect

Comptes Rendus Chimie

www.sciencedirect.com

Preliminary communication/communication

Iron-based nanomaterials used as magnetic mesoporous nanocomposites to catalyze the preparation of *N*-sulfonylimines

Akram Ashouri [a, *], Saadi Samadi [a], Behzad Nasiri [a], Zohre Bahrami [b]

[a] Laboratory of Asymmetric Synthesis, Department of Chemistry, Faculty of Science, University of Kurdistan, 66177-15175, Sanandaj, Iran
[b] Faculty of Nanotechnology, Semnan University, Semnan, 35131-19111, Iran

ARTICLE INFO

Article history:
Received 4 March 2019
Accepted 26 June 2019
Available online 29 July 2019

Keywords:
N-Sulfonylimines
Magnetic mesoporous nanomaterials
Aldimine
Fe_3O_4@MCM-41
Recyclability

ABSTRACT

A new magnetic nanocatalyzed synthetic method for the synthesis of aldimines was evidenced. The reaction was carried out in a Schlenk tube under reflux conditions using various solvents and different nanomaterials as catalysts. In these reactions, an excellent yield of aromatic aldimines was obtained in the presence of silica-coated magnetic nanomaterials. The prepared catalyst was also characterized by Fourier transform infrared spectroscopy, scanning electron microscopy, nitrogen adsorption and desorption studies, energy dispersive X-ray spectroscopy, and small-angle X-ray scattering spectroscopy. It was shown that the magnetic nanocatalysts can be easily separated from the reaction mixture using an external magnet and reused.

1. Introduction

Currently, electron-deficient imines such as sulfonylimines are well known to be important as key intermediates in various chemical reactions [1,2]. Owing to the applicability of these compounds as anticancer agents, their anti-inflammatory nature, and their antibacterial and antifungal behavior, they are also known to be important for biological processes [3]. Owing to their electrophilic nature, relative stability, and reactivity, these electron-deficient imines have been used in the preparation of several important nitrogen-containing compounds [4–6]. Thus, the development and application of suitable methods for imine synthesis have attracted much attention in recent years.

The most widely used and direct method for the preparation of an *N*-sulfonylimine involves the condensation of an aldehyde with sulfonamide, but the low nucleophilic activity of the nitrogen atom of sulfonamide and the difficulty in the removal of the produced water have limited the use of this method [7–9]. To suppress this limitation and increase the efficiency, various methods in the presence of Lewis and Brønsted acids or metal oxides are being developed [10], with some of these suffering from harsh reaction conditions, use of toxic materials, long reaction times, and use of high loading.

Magnetite-based nanomaterials have been used as catalysts for a very wide range of catalytic processes and organic transformations such as coupling reactions [11–13], C–H activation [14], oxidation reactions [15], reduction reactions [16], and synthesis of heterocyclic compounds [17,18]. Therefore, multifunctional nanoparticles are in high demand because of their wide-ranging applications in the field of catalysis. In addition, magnetite nanoparticles are highly desirable for catalytic activity, but under reflux conditions, some aggregation can occur [19,20].

Despite the availability of numerous procedures for the synthesis of imines, the design and development of a new

* Corresponding author.
E-mail address: a.ashouri@uok.ac.ir (A. Ashouri).

https://doi.org/10.1016/j.crci.2019.06.005
1631-0748/

efficient method for the synthesis of aldimines that are more facile and economically advantageous are still of interest. Herein, we attempted to introduce a simple, clean, and efficient process to synthesize aldimines using silica-coated magnetic nanoparticles.

2. Experimental

2.1. Materials

All of the chemicals were obtained from Sigma–Aldrich or Merck and were used without purification. The reaction progress was monitored by thin-layer chromatography (GF254). Fourier transform infrared (FT-IR) (KBr) spectra were recorded using a Bruker Vector 22 FT-IR spectrophotometer. The ^{1}H NMR and ^{13}C NMR spectra were recorded using a Bruker AVIII HD-500 MHz instrument using tetramethylsilane (TMS) as the internal standard.

2.2. Synthesis of different catalysts

The different nanomaterials were synthesized according to reports in the literature [21–24].

2.2.1. Preparation of MCM-41 mesoporous silica

MCM-41 mesoporous silica samples were prepared using a general method [25,26]. The water solution of cetyltrimethylammonium bromide (142 mg, 0.39 mmol) was added to diethanolamine (9.46 mg, 0.09 mmol) and stirred at 40 °C for at least 30 min, followed by the addition of tetraethyl orthosilicate (333 mg, 1.6 mmol) dropwise within 2 min. After 2 h, the solution was cooled to room temperature, and a white residue powder precipitate was obtained that was then centrifuged and washed with ethanol and distilled water. The surfactant cetyltrimethylammonium bromide was extracted from the obtained mesoporous materials by refluxing with ethanol and a small amount of concentrated HCl. The final product was centrifuged and washed with ethanol several times.

2.2.2. Preparation of nanomagnetic Fe_3O_4

Nanomagnetic Fe_3O_4 was prepared using the typical solvothermal method. A round-bottomed flask containing ethylene glycol (30 mL) was filled with ferric chloride hexahydrate (1.48 g, 5.5 mmol) and sodium acetate (2.62 g, 32 mmol). The mixture was heated for 8 h at 200 °C in an autoclave and then cooled to room temperature. The black nanomagnetic Fe_3O_4 was separated using an external magnet, washed with deionized water several times, and dried in an oven at 60 °C overnight [25,26].

2.2.3. Preparation of Fe_3O_4@MCM-41

The procedure for the preparation of Fe_3O_4@MCM-41 was the same as that for nanomagnetic Fe_3O_4 except that in the first step, the prepared MCM-41 (2.0 g) was added to the reaction mixture [29].

2.2.4. General procedure for the synthesis of products

To a Schlenk tube filled with Fe_3O_4@MCM (15 mg) and toluene (0.5 mL), aldehyde (0.12 mmol) and *p*-toluenesulfonamide (17.12 mg, 0.1 mmol) were added under nitrogen atmosphere. The reaction mixture was stirred for 1 h at 100 °C. Then, the silica-coated magnetic nanoparticles were separated using a simple magnet. The solution of the reaction-separated system was transferred into a round-bottomed flask. After the organic phase was evaporated under reduced pressure, the obtained crude product was purified by recrystallization from ethyl acetate and *n*-hexane, affording the pure product in high yield (up to 98%).

***N*-(4-Chlorobenzylidene)-4-methylbenzenesulfonamide** (Table 3, entry 1) mp: 175–179 °C, ^{1}H NMR (500 MHz, $CDCl_3$) δ (ppm): 2.43 (3H, s), 7.35 (d, J = 8.1 Hz, 2H), 7.46 (2H, d, J = 8.5 Hz), 7.86 (2H, d, J = 8.5 Hz), 7.88 (2H, d, J = 8.3 Hz), 8.99 (1H, s); ^{13}C NMR (125 MHz, $CDCl_3$) δ (ppm): 168.6, 144.8, 141.4, 134.8, 132.3, 130.8, 129.8, 129.5, 128.1, 21.6.

***N*-(4-Methylbenzylidene)-4-methyl-benzenesulfonamide** (Table 3, entry 6) mp: 116–118 °C. ^{1}H NMR (500 MHz, $CDCl_3$) δ (ppm): 8.99 (s, 1 H), 7.89 (d, J = 7.5 Hz, 2 H), 7.82 (d, J = 7.4 Hz, 2 H), 7.34 (d, J = 7.49 Hz, 2 H), 7.29 (d, J = 7.43 Hz, 2 H), 2.43 (s, 3 H), 2.42 (s, 3 H); ^{13}C NMR (125 MHz, $CDCl_3$) δ (ppm): 168.9, 145.3, 143.4, 134.4, 130.4 (2C), 128.9 (2C), 128.8, 128.7 (2C), 127.0 (2C), 20.9, 20.6.

***N*-(4-Methoxybenzylidene)-4-methyl-benzenesulfonamide** (Table 3, entry 8) mp: 128–129 °C, ^{1}H NMR (500 MHz, $CDCl_3$) δ (ppm): 8.94 (s, 1 H), 7.87 (d, J = 8 Hz, 4 H), 7.32 (d, J = 7.7 Hz, 2 H), 6.96 (d, J = 8.2 Hz, 2 H), 3.87 (s, 3 H), 2.42 (s, 3 H); ^{13}C NMR (125 MHz, $CDCl_3$) δ (ppm): 168.1, 164.3, 143.2, 134.7, 132.6 (2C), 128.7 (2C), 126.8 (2C), 124.2, 113.6 (2C), 54.6, 20.5.

3. Results and discussion

Initially, in a sealed Schlenk tube under nitrogen atmosphere, the reaction of *p*-chlorobenzaldehyde (**1a**) and *p*-toluenesulfonamide (**2**) was selected as a model reaction in refluxing toluene; but after 24 h, product **3a** was obtained which was not the desired product. Following the reports in the literature, we attempted to carry out the condensation reaction in the presence of catalysts that act as Lewis acids and dehydrating reagents. For this purpose, we carried out the reaction in the presence of several metal oxide nanocatalysts. The obtained results are shown in Table 1. According to entries 2–6, the reaction proceeded in the presence of Al_2O_3, TiO_2, MgO, SiO_2, and Fe_3O_4 metal oxide nanoparticles with moderate yields. On the other hand, owing to its unique properties such as narrow pore size distribution, ultrahigh surface area, well-defined pore structure, and thermal stability, MCM-41 mesoporous silica has been used in several catalytic organic reactions [27–32]. A review of the literature showed that the use of MCM-41 mesoporous silica for the synthesis of aldimines has not been reported. It occurred to us that this class of nanomaterials may be a catalyst for this reaction. When we used MCM-41, the reaction yield increased to 67% (entry 7). To enhance the efficiency of MCM-41 mesoporous silica, we decided to use the silica-coated magnetic nanoparticles denoted as Fe_3O_4@MCM-41 (entry 8). When the reaction was carried out in the presence of Fe_3O_4@MCM-41, the desired product was obtained with the yield of 98% (entry 10). We also used K10 montmorillonite clays as the catalyst

Table 1
Effect of various nanocatalysts on the model reaction.

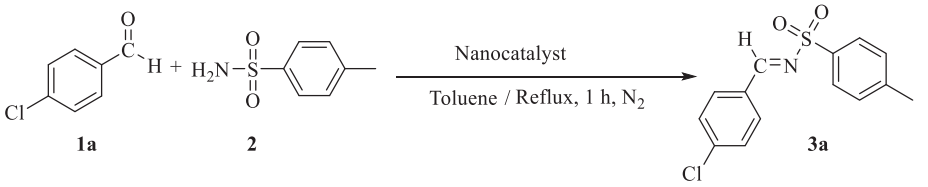

Entry[a]	Type of nanocatalysts	Loading of nanocatalysts (mg)	Yield (%)[b]
1	–	–	–
2	Al_2O_3	15	
3	TiO_2	15	52
4	MgO	15	40
5	Fe_3O_4	15	55
6	SiO_2	15	62
7	MCM-41	15	67
8	Fe_3O_4@MCM-41	15	98
9	K10	15	40
10	Fe_3O_4@MCM-41	5	65
11	Fe_3O_4@MCM-41	10	80
12	Fe_3O_4@MCM-41	20	75
13	Fe_3O_4@MCM-41	25	58

[a] Reaction conditions: *p*-chlorobenzaldehyde (0.12 mmol), *p*-toluenesulfonamide (0.1 mmol), toluene (0.5 mL), and nanocatalysts.
[b] Isolated yield.

under these conditions; but after 1 h, the yield was lower than that obtained using other nanocatalysts (entry 9). Subsequently, we optimized other parameters that affect the reaction. In particular, the effect of different loading amounts of Fe_3O_4@MCM-41 was investigated (entries 10–13). However, it was found that the best yield was achieved using 15 mg of silica-coated magnetic nanocatalysts.

As presented in Table 2, the effect of the solvent was also observed for this reaction. No product was observed using tetrahydrofuran, 1,4-dioxane ,and acetonitrile (entries 1–3). When dichloromethane, chloroform, diethyl ether, and dimethyl sulfoxide were used, the desired aldimine was produced in low to moderate yields (entries 4–7), whereas the use of toluene as solvent promoted the reaction with an extremely high yield (entry 8).

After achieving optimum conditions, the scope of the reaction was evaluated by applying different aldehydes. Several aromatic and aliphatic aldehydes were used, as presented in Table 3. It was found that aromatic aldehydes with an electron-donating group reacted, as did those with electron-withdrawing groups. An aromatic

Table 2
Effect of various solvents on the model reaction.

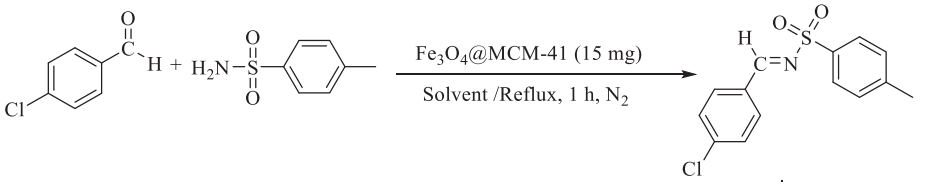

Entry[a]	Solvent	Yield (%)[b]
1	1,4-Dioxane	–
2	Tetrahydrofuran	–
3	Acetonitrile	–
4	Dichloromethane	10
5	Chloroform	20
6	Diethyl ether	35
7	Dimethyl sulfoxide	38
8	Toluene	98

[a] Reaction condition: *p*-chlorobenzaldehyde (0.12 mmol), *p*-toluenesulfonamide (0.1 mmol), solvent (0.5 mL), and Fe_3O_4@MCM-41 (15 mg).
[b] Isolated yield.

Table 3
Reaction scope.

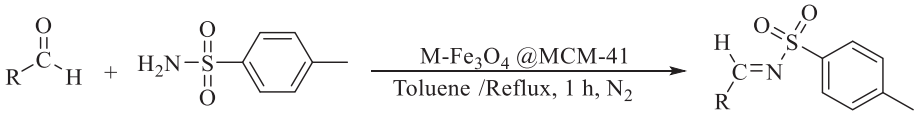

Entry[a]	R	Yield (%)[b]	Mp (°C)	Mp (°C)[c]
1	*p*-Cl-Phenyl	98	175–179	172–173 [33]
2	*o*-Cl-Phenyl	82	134–137	131–132 [34]
3	*m*-Cl-Phenyl	92	84–88	98 [34]
4	*p*-F-Phenyl	88	129–130	117–118 [35]
5	*p*-NO_2-Phenyl	85	203–207	162–170 [35]
6	*p*-CH_3-Phenyl	90	113–115	116–118 [36]
7	*p*-Br-Phenyl	92	190–193	198–199 [37]
8	*p*-OCH_3-Phenyl	87	129–130	128–129 [35]
9	*o*–OCH_3-Phenyl	85	111–114	111–113 [38]
10	*p*-CF_3-Phenyl	90	154–156	159–160 [39]
11	-Phenyl	86	79–82	105–108 [35]
12	-Naphthyl	89	140–144	142–144 [40]
13	-Anthracyl	82	199–204	214–217 [41]
14	-Benzyl	Oily mixture	–	–
15	-Hexyl	Oily mixture	–	–
16	-Propenyl	Oily mixture	–	–

[a] Reaction conditions: aldehyde (0.12 mmol), *p*-toluenesulfonamide (0.1 mmol), toluene (0.5 mL), and Fe_3O_4@MCM-41 (15 mg).
[b] Isolated yield.
[c] Reported Mp.

aldimine substituted with bulky aryl groups was synthesized in high yields (entries 12 and 13). As expected, aromatic aldehydes reacted better than the aliphatic aldehydes (entries 14–16). In nearly all of the investigated reactions, the conversion was over 95% under the reaction conditions.

3.1. Characterization of materials

The prepared materials were characterized using a Bruker Vector 22 FT-IR spectrophotometer. The surface morphology of the samples was examined using a ZEISS SIGMA VP field emission scanning electron microscope (FE-SEM) equipped with a field emission gun and an energy dispersive (EDS) detector. The surface areas were calculated according to the Brunauer–Emmett–Teller (BET) equation and the pore size distribution was calculated using the Barrett–Joyner–Halenda (BJH) equation. Elemental analysis was performed quantitatively using an Infinite 200 PRO NanoQuant instrument (Tecan, Switzerland). The nanoscale density differences were evaluated by small-angle X-ray scattering (SAXS) spectroscopy.

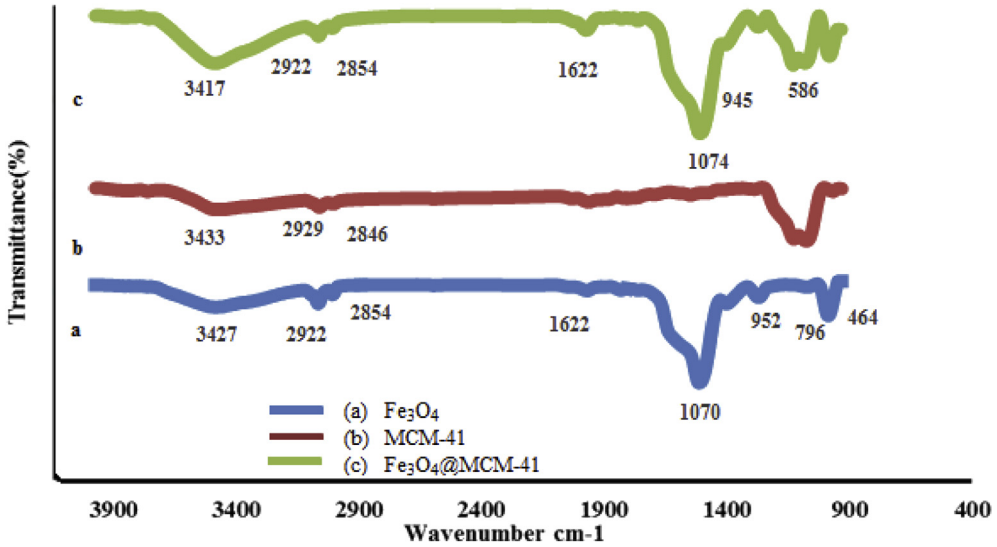

Fig. 1. FT-IR spectra of (a) MCM-41, (b) Fe_3O_4, and (c) Fe_3O_4@MCM-41.

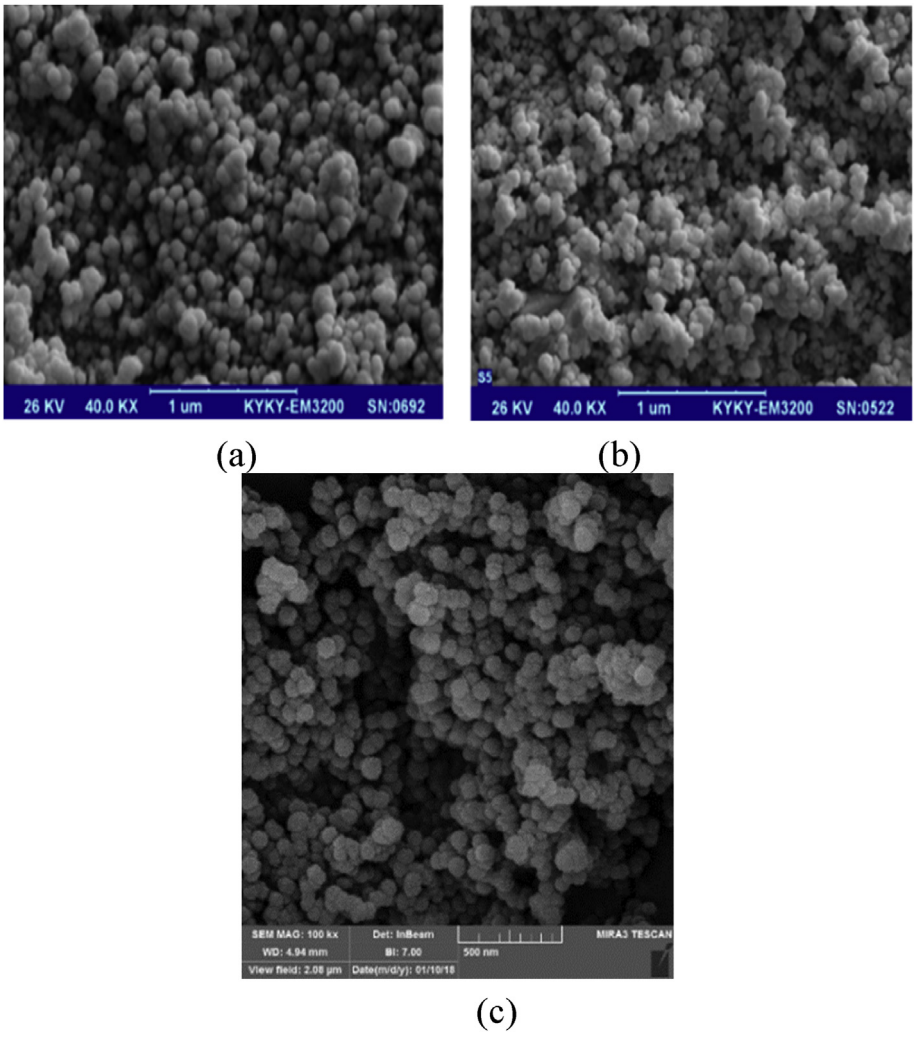

Fig. 2. SEM images of (a) Fe_3O_4, (b) MCM-41, and (c) Fe_3O_4@MCM-41.

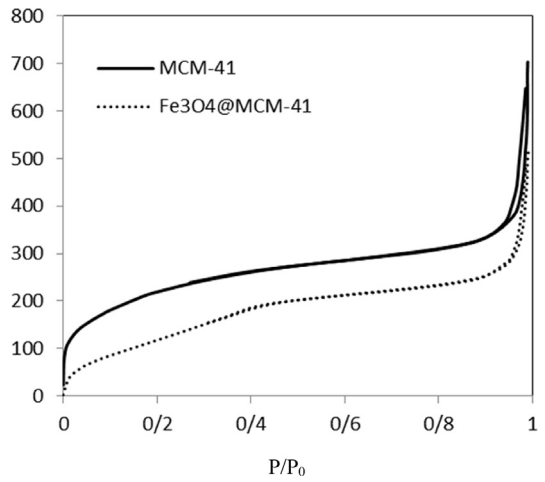

Fig. 3. N_2 adsorption/desorption isotherm of MCM-41 and Fe_3O_4@MCM-41 nanoparticles.

Table 4
Textural properties of MCM-41 and Fe_3O_4@MCM-41 nanoparticles.

Sample	Specific surface area (S_{BET}) ($m^2\ g^{-1}$)	Pore volume (V_p) ($cm^3\ g^{-1}$)	Pore diameter (D_p) (nm)
MCM-41 nanoparticles	817	1.068	2.42
Fe_3O_4@MCM-41 nanoparticles	690	0.873	2.42

3.2. Composition and morphology of Fe_3O_4, MCM-41, and Fe_3O_4@MCM-41

The FT-IR spectra of the prepared MCM-41, Fe_3O_4, and Fe_3O_4@MCM-41 are shown in Fig. 1. The asymmetric and symmetric stretching vibrations of the siloxane groups (Si—O—Si) of MCM-41 are ascribed to the bands at 1074 and 796 cm^{-1} that are observed to be unchanged in

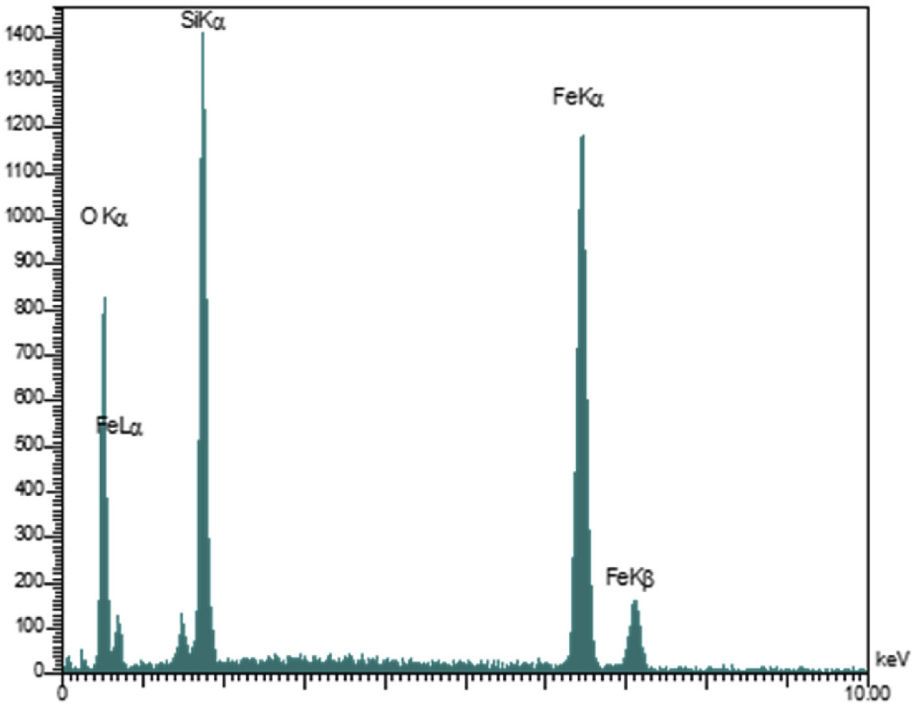

Fig. 4. EDX spectrum of Fe_3O_4@MCM-41.

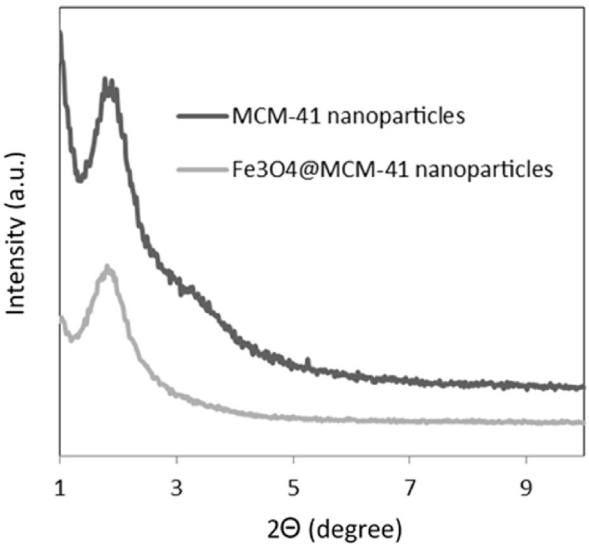

Fig. 5. SAXS patterns of MCM-41 and Fe_3O_4@MCM-41 nanoparticles.

Fe_3O_4@MCM-41. The strong absorption band related to the Fe–O bond observed at approximately 586 cm^{-1} in the Fe_3O_4 and Fe_3O_4@MCM-41 spectra confirms the preparation and the presence of magnetite nanoparticles, respectively.

The surface morphologies of Fe_3O_4, MCM-41, and Fe_3O_4@MCM-41 were observed by scanning electron microscopy (SEM) and are shown in Fig. 2. Bare Fe_3O_4 nanoparticles have a quasi-spherical shape with a heterogeneous surface and slight aggregation. The shape of the resulting silica-coated magnetic nanoparticles was also spherical after grafting on MCM-41. These results indicated that Fe_3O_4 nanoparticles were successfully grafted on the MCM-41 nanoparticles without considerable changes during the functionalization process.

N_2 adsorption–desorption isotherms and pore size distributions of MCM-41 and Fe_3O_4@MCM-41 silica-coated magnetic nanoparticles are shown in Fig. 3. The isotherms and pore size distributions of MCM-41 magnetic mesoporous silica and corresponding silica-coated magnetic nanoparticles are nearly same, indicating that the pore structures of the MCM-41 mesoporous silica were still preserved even after the grafting of Fe_3O_4 nanoparticles on the MCM-41 mesoporous silica. The textural properties of MCM-41 and Fe_3O_4@MCM-41 nanoparticles are summarized in detail in Table 4. It is clear that the surface area and pore volume of silica-coated magnetic nanoparticles were lower than those of the MCM-41 mesoporous silica; however, the surface areas and large pore volumes of the Fe_3O_4@MCM-41 nanoparticles are still high.

Fig. 4 shows the energy-dispersive X-ray (EDX) spectrum of the obtained Fe_3O_4@MCM-41 nanoparticles that reveals the presence of Fe, O, and Si elements, confirming that MCM-41 was successfully coated by magnetite nanoparticles.

The small angle X-ray scattering (SAXS) patterns of MCM-41 and silica-coated magnetic nanoparticles are presented in Fig. 5 and are in good agreement with those

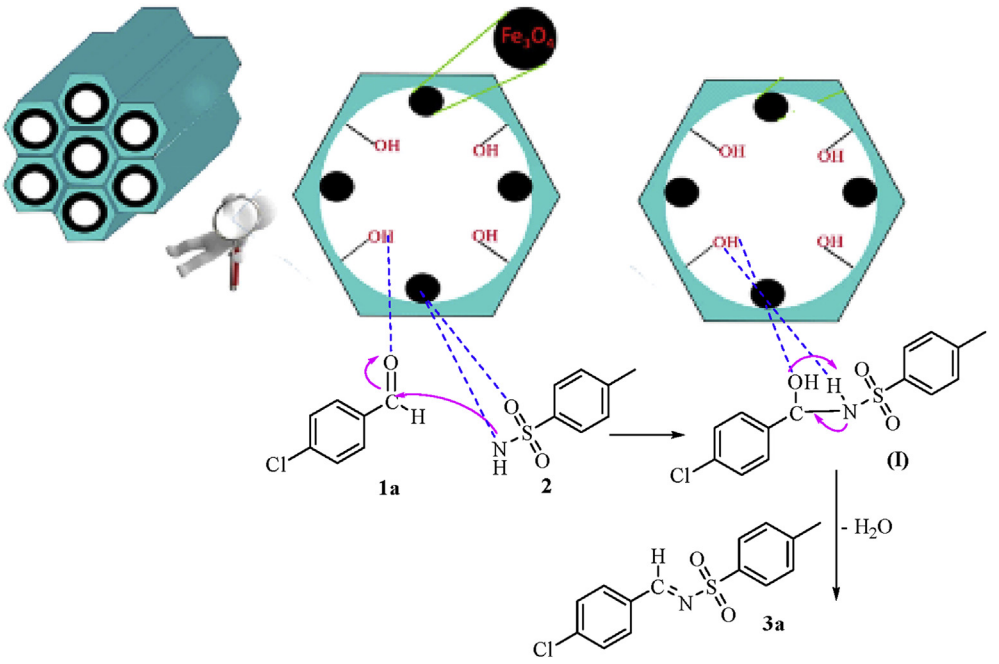

Scheme 1. Proposed mechanism for the synthesis of aldimine derivatives in the presence of silica-coated magnetic nanoparticles.

reported in the literature [42]. The SAXS pattern of the silica-coated magnetic nanoparticles was almost identical to that of the corresponding mesoporous silica. This result also supports the conclusion that the pore structures of mesoporous silica were preserved even after the grafting of Fe_3O_4 nanoparticles.

3.3. Proposed mechanism

A proposed mechanism for the synthesis of aldimine derivatives in the presence of silica-coated magnetic nanoparticles is shown in Scheme 1. After activation of the aldehyde carbonyl group by Fe_3O_4@MCM-41, the nucleophilic attack of the nitrogen atom of sulfonamide occurred, and an intermediate (I) was formed. Consequently, the aldimine product **3a** was prepared by the dehydration of the intermediate (I).

3.4. Recyclability and reusability of the catalyst

Recyclability and reusability of the catalyst are important for designing a new synthesis method. Therefore, the reusability of the silica-coated magnetic nanoparticles was also evaluated for the condensation reaction. The conversion and yield of the reaction were over 90% and 83%, respectively, until five cycles, demonstrating that the catalytic activity of the silica-coated magnetic nanoparticles was preserved without a significant loss (see Fig. 6). After each reaction, magnetic nanocatalysts were simply separated by an external magnet, washed with ethanol, dried under reduced pressure and reused. The FT-IR spectrum and SEM image of the recycled catalyst confirmed that the structure of the catalyst was maintained.

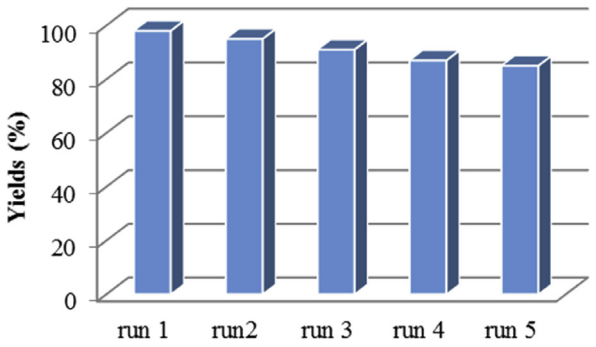

Fig. 6. Effect of catalyst recycling on the yield of product **3a**.

4. Conclusions

In this work, a simple and new synthetic method of silica-coated magnetic nanoparticles via the condensation of aldehyde and *p*-toluenesulfonamide using silica-coated iron-based magnetic nanoparticles was introduced. The synthesis of aldimines was carried out in a Schlenk tube that can be easily handled in comparison with a Dean–Stark apparatus. The excellent yield of aromatic aldimines, short reaction time, facile separation, reusability of catalysts, and lack of catalyst pollution in the products are the prominent advantages of this method.

Acknowledgements

We are grateful to the University of Kurdistan, Iran Research Councils for the support of this work.

Appendix A. Supplementary data

Supplementary data to this article can be found online at https://doi.org/10.1016/j.crci.2019.06.005.

References

[1] M.E. Belowich, J.F. Stoddart, Chem. Soc. Rev. 41 (2012) 2003–2024.
[2] A. Kajal, S. Bala, S. Kamboj, N. Sharma, V. Saini, J. Catal. 2013 (2013).
[3] A.T. Baviskar, U.C. Banerjee, M. Gupta, R. Singh, S. Kumar, M.K. Gupta, S. Kumar, S.K. Raut, M. Khullar, S. Singh, Bioorg. Med. Chem. 21 (2013) 5782–5793.
[4] J.L. Garcia Ruano, J. Alemán, M. Belen Cid, A. Parra, Org. Lett. 7 (2005) 179–182.
[5] A. Vass, J. Dudás, R.S. Varma, Tetrahedron Lett. 40 (1999) 4951–4954.
[6] L. Wu, X. Yang, X. Wang, F. Yan, J. Sulfur Chem. 31 (2010) 509–513.
[7] S. Nakamura, M. Hayashi, Y. Hiramatsu, N. Shibata, Y. Funahashi, T. Toru, J. Am. Chem. Soc. 131 (2009) 18240–18241.
[8] S. Kobayashi, Y. Mori, J.S. Fossey, M.M. Salter, Chem. Rev. 111 (2011) 2626–2704.
[9] R.N. Ram, A.A. Khan, Synth. Commun. 31 (2001) 841–846.
[10] J.H. Wynne, S.E. Price, J.R. Rorer, W.M. Stalick, Synth. Commun. 33 (2003) 341–352.
[11] Y. Long, K. Liang, J. Niu, X. Tong, B. Yuan, J. Ma, New J. Chem. 39 (2015) 2988–2996.
[12] W. Li, Y. Tian, B. Zhang, L. Tian, X. Li, H. Zhang, N. Ali, Q. Zhang, New J. Chem. 39 (2015) 2767–2777.
[13] J. Niu, F. Wang, X. Zhu, J. Zhao, J. Ma, RSC Adv. 4 (2014) 37761–37766.
[14] R. Sharma, S. Dutta, S. Sharma, Dalton Trans. 44 (2015) 1303–1316.
[15] L. Lykke, C. Rodríguez-Escrich, K.A. Jørgensen, J. Am. Chem. Soc. 133 (2011) 14932–14935.
[16] T.C. Nugent, M. El-Shazly, Adv. Synth. Catal. 352 (2010) 753–819.
[17] A.V. Kel'in, A.W. Sromek, V. Gevorgyan, J. Am. Chem. Soc. 123 (2001) 2074–2075.
[18] Y.-L. Shi, M. Shi, Org. Biomol. Chem. 5 (2007) 1499–1504.
[19] W. Xie, J. Wang, Energy Fuel. 28 (2014) 2624–2631.
[20] W. Xie, X. Zang, Food Chem. 194 (2016) 1283–1292.
[21] B. Li, X. Wang, M. Yan, L. Li, Mater. Chem. Phys. 78 (2003) 184–188.
[22] F. Liu, M.M. Abed, K. Li, J. Membr. Sci. 366 (2011) 97–103.
[23] C.H. Kwon, J.H. Kim, I.S. Jung, H. Shin, K.H. Yoon, Ceram. Int. 29 (2003) 851–856.
[24] Z.-X. Tang, L.-E. Shi, Ecletica Quim. 33 (2008) 15–20.
[25] W. Xie, Y. Han, H. Wang, Renew. energ. 125 (2018) 675–681.
[26] S. Luo, G. Fan, M. Luo, J. Li, G. Song, J CO_2 UTIL 14 (2016) 23–30.
[27] S.C. Tang, I.M. Lo, Water Res. 47 (2013) 2613–2632.
[28] A. Yan, X. Liu, G. Qiu, H. Wu, R. Yi, N. Zhang, J. Xu, J. Alloy. Comp. 458 (2008) 487–491.
[29] S.V. Kolotilov, O. Shvets, O. Cador, N. Kasian, V.G. Pavlov, L. Ouahab, V.G. Ilyin, V.V. Pavlishchuk, J. Solid State Chem. 179 (2006) 2426–2432.
[30] M. Vallet-Regi, A. Ramila, R. Del Real, J. Pérez-Pariente, Chem. Mater. 13 (2001) 308–311.
[31] K. Chaudhari, T. Das, P. Rajmohanan, K. Lazar, S. Sivasanker, A. Chandwadkar, J. Catal. 183 (1999) 281–291.
[32] X. Zhao, G. Lu, X. Hu, Microporous Mesoporous Mater. 41 (2000) 37–47.
[33] C.-Y. Chen, H.-X. Li, M.E. Davis, Microporous Mater. 2 (1993) 17–26.
[34] S. Samadi, K. Jadidi, B. Khanmohammadi, N. Tavakoli, J. Catal. 340 (2016) 344–353.
[35] S. Samadi, A. Ashouri, M. Ghambarian, RSC Adv. 7 (2017) 19330–19337.
[36] T.S. Jin, M.J. Yu, L.B. Liu, Y. Zhao, T.S. Li, Synth. Commun. 36 (2006) 2339–2344.
[37] R. Patel, V.P. Srivastava, L.D.S. Yadav, Adv. Synth. Catal. 352 (2010) 1610–1614.
[38] D. Huang, X. Wang, X. Wang, W. Chen, X. Wang, Y. Hu, Org. Lett. 18 (2016) 604–607.
[39] A. Zare, F. Bahrami, M. Merajoddin, M. Bandari, A.R. Moosavi-Zare, M.A. Zolfigol, A. Hasaninejad, M. Shekouhy, M.H. Beyzavi, V. Khakyzadeh, Org. Prep. Proced. Int. 45 (2013) 211–219.
[40] M.D. Hopkins, K.A. Scott, B.C. DeMier, H.R. Morgan, J.A. Macgruder, A.A. Lamar, Org. Biomol. Chem. 15 (2017) 9209–9216.
[41] A.K. Bhattacharya, K.C. Rana, C. Pannecouque, E. De Clercq, ChemMedChem 7 (2012) 1601–1611.
[42] C.-J. Wang, M. Shi, J. Org. Chem. 68 (2003) 6229–6237.